Pergamon

Journal of Structural Geology, Vol. 16, No. 3, pp. 355 to 370, 1994

0191-8141/94 $06.00+0.00

Contrasting styles of deformation during progressive nappe stacking at the southeastern margin of the Bohemian Massif (Thaya Dome)

KAREL SCHULMANN and RADEK MELKA

Department of Petrology, Charles University, Albertov 6, 128 43 Praha 2, Czechoslovakia

MICHAL Z LOBKOWICZ

Czech National Council, Sněmovní 4, 110 00 Praha 1, Czechoslovakia

PATRICK LEDRU

Bureau de Recherches Géologiques et Minières, BP 6009, Avenue de Concyr, F-45060 Orléans Cédex, France

JEAN-MARC LARDEAUX

Laboratoire des Sciences de la Terre, Ecole Normale Supérieure de Lyon, 46 Allée d'Italie, F-69364 Lyon Cédex 07, France

and

ALBERT AUTRAN

Bureau de Recherches Géologiques et Minières, BP 6009, Avenue de Concyr, F-45060 Orléans Cédex, France

(*Received* 17 *February* 1992; *accepted in revised form* 19 *April* 1993)

Abstract—Variscan nappe stacking at the southeastern margin of the Bohemian Massif is a polyphase process implying a progressive modification of the deformation regime from thrusting to wrenching, associated change of finite strain axes orientations and progressive downwards migration of thrust, or wrench, planes. A first high-temperature deformation phase (D_1) is related to nappe stacking of Moldanubian units in a NW–SE direction; it is recorded only in these units. D_2 corresponds to the piling of the Moldanubian units over the Moravian ones producing internal nappe stacking of the latter and a first medium-temperature mylonitization of Thaya basement rocks. The main feature of this stage is a switch in finite strain axes orientation and northeastward transpressional shearing. Strain partitioning is important within the Moravian nappes and implies alternation of plane strain, oblate, and constrictional, fabrics. D_3 is also a phase connected with strong non-coaxial NE-directed shearing. It is concentrated in zones of weakness and causes reactivation of older structures. The structural pattern strongly depends on the position in the nappe pile: strike-slip tectonics dominate near the resistant eastern Cadomian basement border, foliation-parallel extensional reactivation producing large-scale folds is typical in Moravian nappes, while extensional tectonics prevail in the uppermost Gföhl nappe. Large-scale strain partitioning during D_2 stacking of Moravian nappes and the extension of the upper part of the nappe pile during D_3 reactivation are mechanically controlled by a lateral ramp basement geometry along the Bruno-Vistulian Cadomian foreland.

INTRODUCTION

THE eastern margin of the Bohemian Massif corresponds to the front of the Variscan collisional belt where it is in contact with the Cadomian continental block (Bruno-Vistulian basement) (Fig. 1a). Here, the thrust units are stretched in a NE–SW direction, parallel to the ancient continental margin (Rajlich 1987, Schulmann *et al.* 1991). Structural data support a polyphase stacking of nappes, evolving from thrusting to wrenching. A dominant role in shaping of the resulting structures is played by the lateral-ramp geometry of (para) autochthonous units. The aims of this contribution are: (1) to describe the lithotectonic zonation of the Variscan nappe pile at the southeastern margin of the Bohemian Massif; (2) to define the polyphase syn-metamorphic stacking of thrust sheets connected with the Variscan convergence; and (3) to characterize the contrasting styles of reactivation of the autochthonous and lower— and upper—allochthonous units during late tectonic movements.

MAIN LITHOTECTONIC ZONATION OF THE NORTHERN TERMINATION OF THE THAYA DOME

The crystalline complexes at the eastern margin of the Bohemian Massif have been subdivided by Suess (1912,

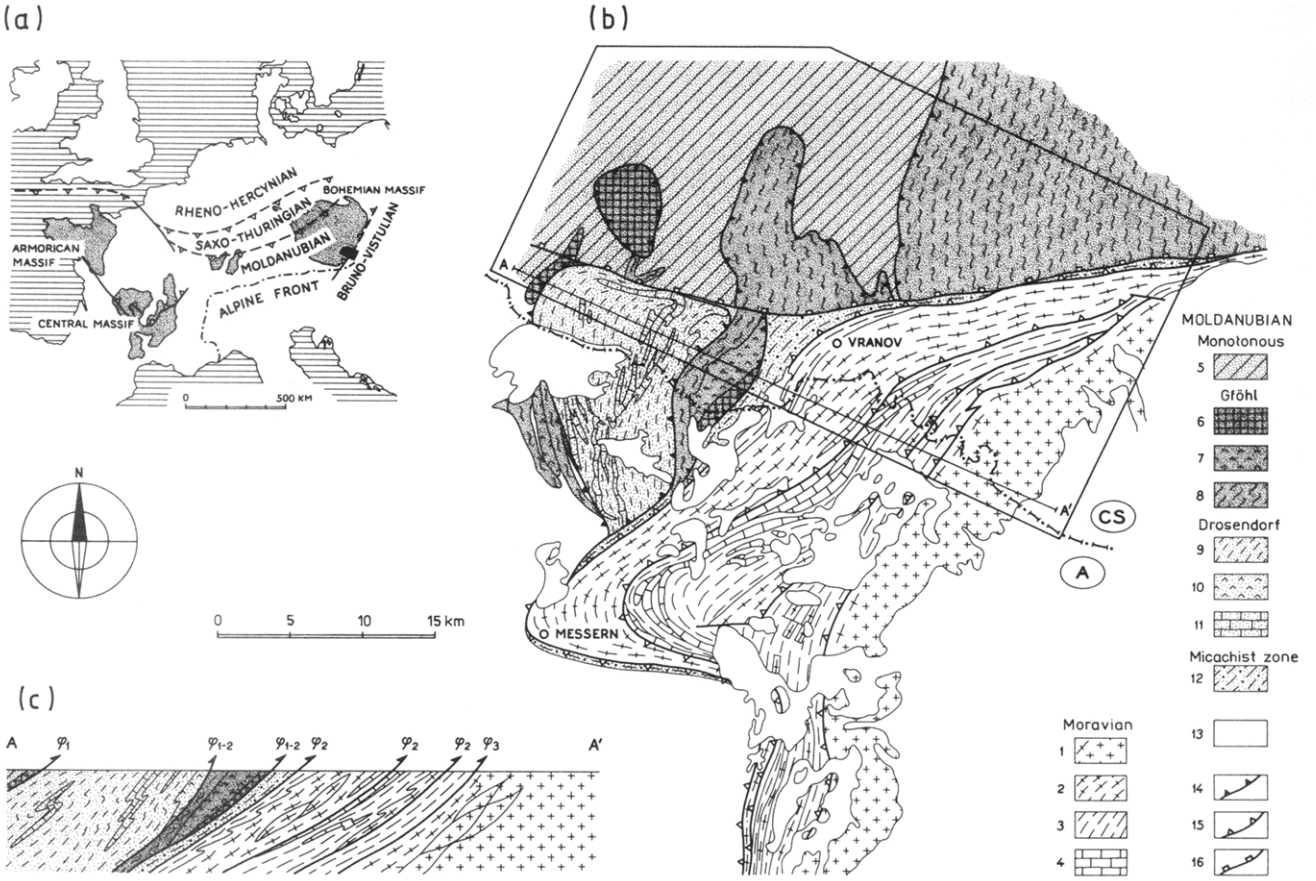

Fig. 1. (a) Position of the studied area in the European Variscides. (b) Geological map of the studied area (after Frasl et al. 1977). (c) NW–SE cross-section with indicated D_1, D_2 and D_3 thrust–wrench planes. 1, Thaya granite; 2, Bíteš and Weitersfeld orthogneisses; 3, phyllites (Outer Phyllites, Pleissing nappe and roof of Thaya granite); 4, calc-silicate rocks of Pleissing nappe; 5, Monotonous nappe; 6, Gföhl granulites; 7, anatectic granite; 8, migmatities; 9, metapelites; 10, amphibolites; 11, marbles; 12, mica-schist zone; 13, Neogene; 14, D_1 thrusts; 15, D_{2-3} thrust–wrench planes; 16, normal fault.

1926) into two principal units, Moldanubicum and Moravicum, which differ in metamorphic grade and style of deformation (Fig. 1b). According to this concept the Moldanubicum, consisting of high-grade metamorphic rocks, has been overthrust on medium-grade Moravian crystalline rocks which appear now as a large-scale tectonic window called the Thaya Dome. Three main zones are defined in the Thaya Dome area (Preclik 1925, 1926). From top to bottom (or from west to east) these are the Moldanubian zone, the Moravian zone and the Bruno-Vistulian basement (Figs. 1b & c and 2).

The Moldanubian zone, composed of high-grade rocks with relics of high-pressure metamorphism, is divided into four units: the Gföhl, Monotonous and Drosendorf nappes, and the Micaschist zone.

The Gföhl nappe consists of sillimanite- and garnet-bearing banded paragneisses associated with numerous intercalations of calc-silicate rock, marble, amphibolite, eclogite and felsic granulite (Matějovská 1975). The significance of partial melting increases towards the east where anatexites and leucocratic migmatites dominate.

The Monotonous nappe consists of biotite–sillimanite paragneisses with intercalations of quartzite and amphibolite. Granulite bodies are rare.

The Drosendorf nappe contains a sequence of paragneiss, amphibolite, marble, calc-silicate rock, quartzite and graphite-bearing schists (Jenček & Dudek 1971). In its lower part there is a typical leptynoamphibolite complex of several hundred metres in thickness. Relics of high-pressure metamorphism are so far unknown. The base of this nappe is marked by a NW-trending syntectonic intrusion of leucocratic anatectic peraluminous granite. Structurally below the Drosendorf nappe lies a tectonic slice of Gföhl granulite and metagabbro.

The Micaschist zone represents the most important interface between the Moldanubian and Moravian zone (Suess 1912, 1926, Johan *et al.* 1990, Schulmann *et al.* 1991). It consists mainly of garnet–kyanite–staurolite micaschist that includes some garnet–amphibolite bodies. In the northern part of the Moravian zone, the existence of an early high-pressure metamorphic stage is shown by the presence of talc–kyanite assemblages and relics of staurolite–chloritoid in almandine (Lardeaux *et al.* 1991).

The Moravian zone lies structurally below the allochthonous Moldanubian terrane. Two large-scale nappe structures have been distinguished within the Moravian zone (Preclik 1925, Waldmann 1930); the Bíteš orthogneiss nappe and the Pleissing nappe.

The Bíteš orthogneiss nappe (Figs. 1 and 2) consists of leucocratic Bíteš orthogneiss and its country rock, the Outer Phyllite unit. The protolith of the orthogneiss was

probably of Cadomian age as is indicated by divergent Rb–Sr dates of 790 Ma (Scharbert 1977) and 560 Ma (Morauf & Jäger 1982). In its upper part, numerous intrusions of sheeted sills of the Bíteš orthogneiss penetrate a varied metasedimentary succession of the Outer Phyllite unit, proving its intrusive character. The Outer Phyllite unit contains numerous intercalations of calc-silicate rock, tremolitic (commonly graphitic) marble, quartzite, garnet amphibolite and rarely garnet–kyanite–staurolite micaschist.

The Pleissing nappe (Figs. 1 and 2) consists of metapelite and numerous intercalations of impure marble, calc-silicate rock (Fugnitzer Kalksilikatschiefer) and amphibolite. The strongly deformed body of Weitersfeld orthogneiss lies at the base of the nappe. Sheets of Weitersfeld orthogneiss cut the metapelitic roof, the structures of the orthogneiss and host rock being presently concordant (Preclik 1926).

The Bruno-Vistulian basement (Dudek 1980) is represented by mostly granitic to granodioritic Thaya plutonic complex (Figs. 1 and 2) of Cadomian age (550 Ma, Rb–Sr, Scharbert & Batík 1985). Metasedimentary rocks at the roof of the Thaya granite are interpreted to be the original host rock of the Thaya granite (Preclik 1925, 1926, Frasl *et al.* 1977, 1990, Frasl 1983). It is composed of biotite–garnet micaschist, metagraywacke, hornfels and hornfels–quartzite; rare migmatites were described by Preclik (1926) and Hájek (1990). Similar rocks form N–S-trending xenoliths in the central part of the Thaya granite. Thus, the metasedimentary rock in the roof of the Thaya granite exhibits remnants of late Proterozoic amphibolite facies metamorphism (Preclik 1926, Frasl 1983). Along the easternmost part of the Thaya granite, the transgressive Devonian sedimentary cover is preserved (Dudek 1960).

TECTONIC EVOLUTION OF THE EASTERN MARGIN OF THE BOHEMIAN MASSIF

Main features of the tectonic evolution of the area were described by Suess (1912) in his concept of eastward overthrusting of a high-grade Moldanubian slab over the Moravian foreland producing classical inverted

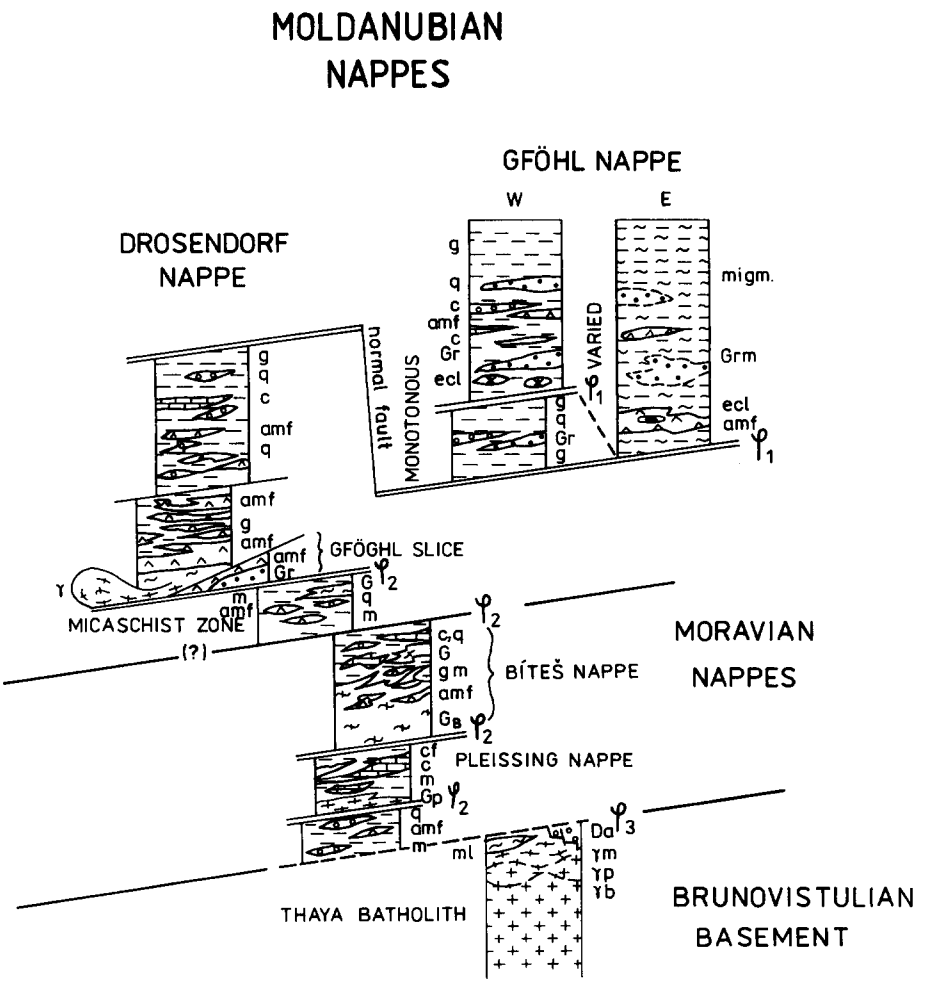

Fig. 2. Lithostratigraphic zonation in the southeastern margin of the Bohemian Massif. g, biotite–sillimanite paragneiss; migm, migmatites; amf, amphibolite; q, quartzite; c, marble; gr, granulite; grm, migmatized granulite; ecl, eclogite; m, micaschist; G, orthogneiss; Gb, Bíteš orthogneiss; Gp, Weitersfeld orthogneiss; cf, calc-silicate rocks; γm, mylonitized granite; γp, heterogenously deformed granite; γb, undeformed biotite granite; mi, Cadomian migmatite; Da, Devonian clastics; φ_1, D_1 thrust zones in the Moldanubian nappe pile; φ_2, D_2 thrust zones in the Moravian nappe pile including the Moldanubian thrust; φ_3, D_3 shear zone separating the para-autochthonous metasedimentary roof of the Thaya batholith from the basement rocks.

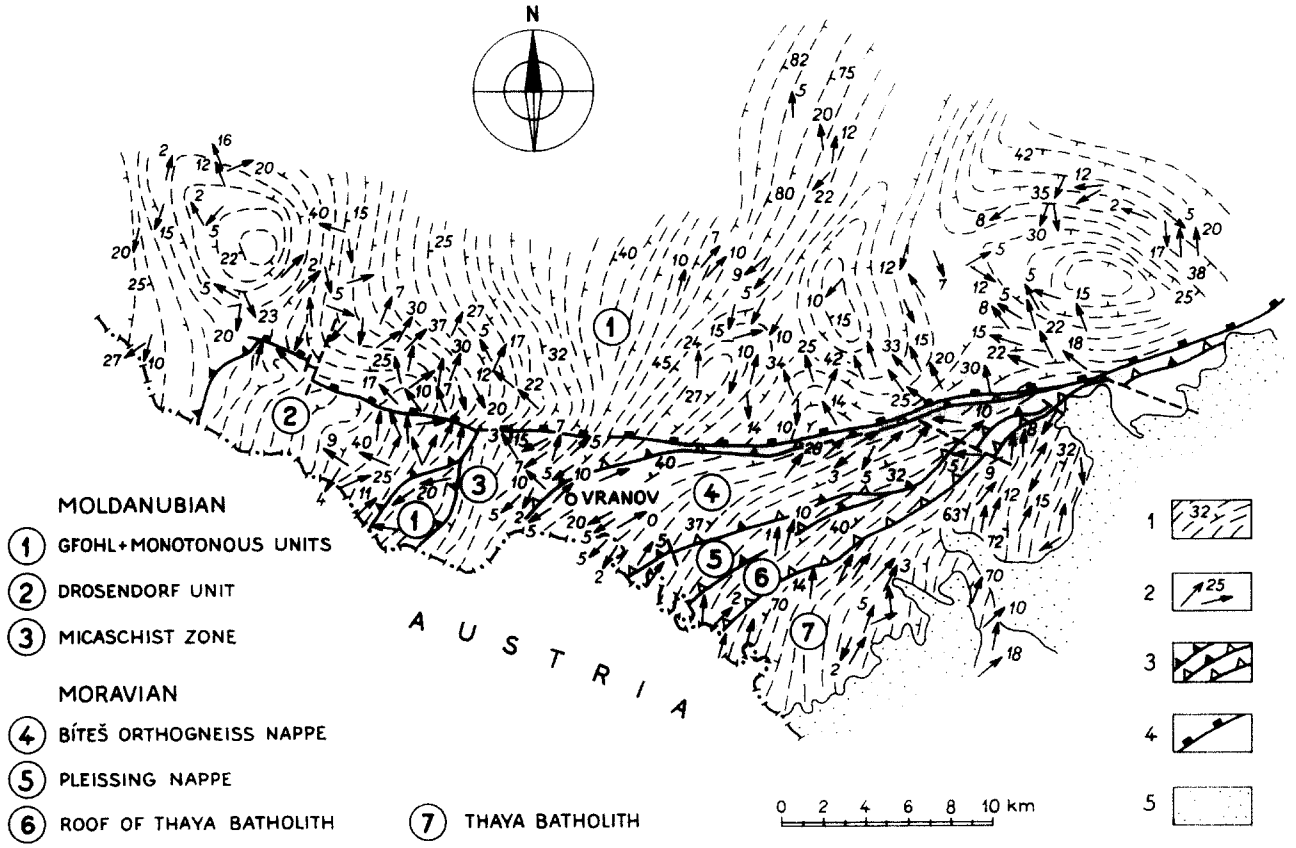

Fig. 3. Foliation, stretching and mineral lineation map. (1) Metamorphic foliation S_1 and S_2 (undistinguished). (2) Stretching lineation L_1 and L_2 (undistinguished). (3) Thrust–wrench boundaries (D_1, D_2, D_3, respectively). (4) Normal fault boundary. (5) Neogene.

medium-grade metamorphism in Moravian rocks. However, Suess's (1912) kinematic model is based on the interpretation of stretching lineations to be perpendicular to the main tectonic transport direction ('B- tectonite'; Sander 1911, 1930); he also considered the tectonic reworking of the Moravian zone as monophase. Our data indicate a more complicated tectonic and kinematic evolution of the Moldanubian–Moravian collisional zone.

Three major deformation phases have been recognized. The first tangential deformational phase (D_1) corresponds to internal shearing within the Moldanubian zone (stacking of the Gföhl, Monotonous and Drosendorf nappes). It was followed by D_2 movements parallel to the plate boundary in the Moravicum and the basement (transpressional deformation) and by late reactivation (D_3) that affected the whole nappe pile. D_1 and D_2 phases are syn-metamorphic and D_3 is essentially a phase of deformation during retrograde metamorphism.

FIRST DEFORMATION PHASE (D_1)

The oldest recognizable deformation D_1 in the Moldanubicum (Gföhl, Monotonous and Drosendorf nappes) was synchronous with HT–MP metamorphism. In the Gföhl nappe, relics of HP metamorphism (high-temperature eclogite and garnet peridotite) document a pre-D_1 metamorphic history (Medaris *et al.* 1990). A flat-lying S_1 foliation (Fig. 3) is outlined in paragneiss by alternating mica-rich layers and pockets of anatectic melt, whereas in granulite and orthogneiss it is marked by quartz ribbons and mica alignment. A NW-trending mineral lineation L_1 (Figs. 3 and 4) is mostly marked by elongate quartz–feldspar, micaceous and sillimanite aggregates in all rock types.

The orientation of rootless recumbent F_1 fold axes is irregular in trend, but a dominant NW trend is present (Fig. 5). These folds are isoclinal and purely similar in geometry with very acute shape. Symmetrical 'chocolate-tablet' lenticular boudins of amphibolite, eclogite and calc-silicate rock suggest a predominantly coaxial deformation. The significant separation of individual boudins in both XY and YZ sections indicates 100–600% shortening.

Despite the predominantly coaxial component of deformation, rare kinematic shear criteria such as melt-filled NW- or SE-dipping shear-bands (Platt & Vissers 1980) and asymmetrical boudins in calc-silicate rocks are present. In most cases they indicate a southeasterly displacement direction.

D_2 STRUCTURES

The definition of a D_2 tectonic phase, affecting the whole nappe pile, is based on the coherence of the

orientation of principal axes of finite strain; style of folding and kinematics consistently indicate top-to-the-northeast displacement. D_2 is the first deformation phase which affects the Moravian nappe, but the second one in the Moldanubicum, where D_2 structure geometry, kinematics, deformation and *PT* regime differ from that of D_1 deformation.

First reactivation of the Moldanubian pile

In many places within the upper allochtonous Moldanubian nappes, early D_1 NW–SE structures were overprinted by D_2 deformation. A change in bulk kinematics during D_2 is shown by the NE–SW trend of L_2 lineations, perpendicular to the trend of D_1 structures. L_2 is marked by the growth of sillimanite fibres and aligned biotite.

S_2 is either flat-lying and subparallel to S_1 planes in the eastern and western parts of the studied area, or almost subvertical with a NNE–SSW trend in the central strike-slip zone (Fig. 3). High- to medium-temperature mylonitization and foliation reactivation is characteristic of D_2 deformation.

D_2 reworking is most intense in the lowermost Moldanubian Drosendorf nappe where several NW-dipping mylonite zones affect anatectic granite at the base of the unit and adjacent micaschists and amphibolites. Subhorizontal F_2 sheath folds with NE-trending noses (Cobbold & Quinquis 1980) deform S_1 (Fig. 6a) and are connected with an intense heterogeneous dextral shearing. Close to tight NW-vergent asymmetric folds with axes parallel to the L_2 lineation (Fig. 5), are intimately connected with sheath folds. NW–SE-trending neck-zones between barrel-shaped boudins of rigid amphibolite layers embedded in banded gneiss confirm the change in orientation of bulk finite strain ellipsoid during D_2 (Fig. 7a).

D_2 kinematic criteria throughout the Moldanubian nappe such as shear bands (Platt & Vissers 1980) and *S–C* fabrics (Berthé *et al.* 1979) indicate top-to-the-northeast movement (dextral in the central strike-slip zone) (Figs. 8a–c).

D_2 *deformation in the Moravian zone*

The first deformation phase recognized in the Moravian nappes was contemporaneous with amphibolite facies metamorphism and corresponds to D_2 defor-

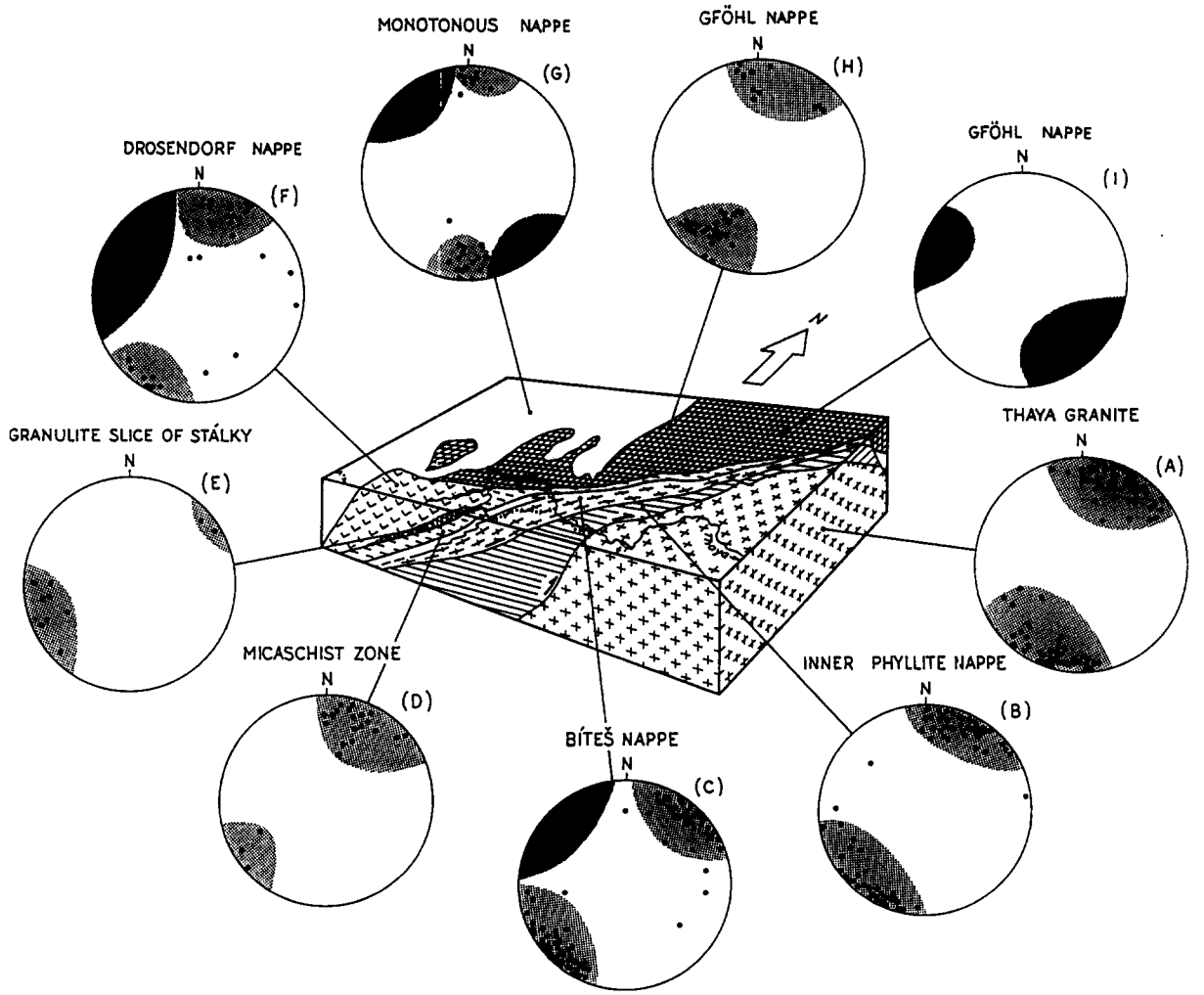

Fig. 4. Orientation diagrams of L_1 and L_2 stretching lineations. Lower-hemisphere equal-area projections. NW-trending L_1 lineations (dark-shaded areas in the stereograms) predominate in the Gföhl nappe (I), the Monotonous nappe (G) and the Drosendorf nappe (F). NE-trending lineation L_2 (light-shaded areas) prevails in basement (A), the Moravian nappes (B) and (C) and the micaschist zone (D), and is also found in the Gföhl (E), (H) and Drosendorf (F) nappes.

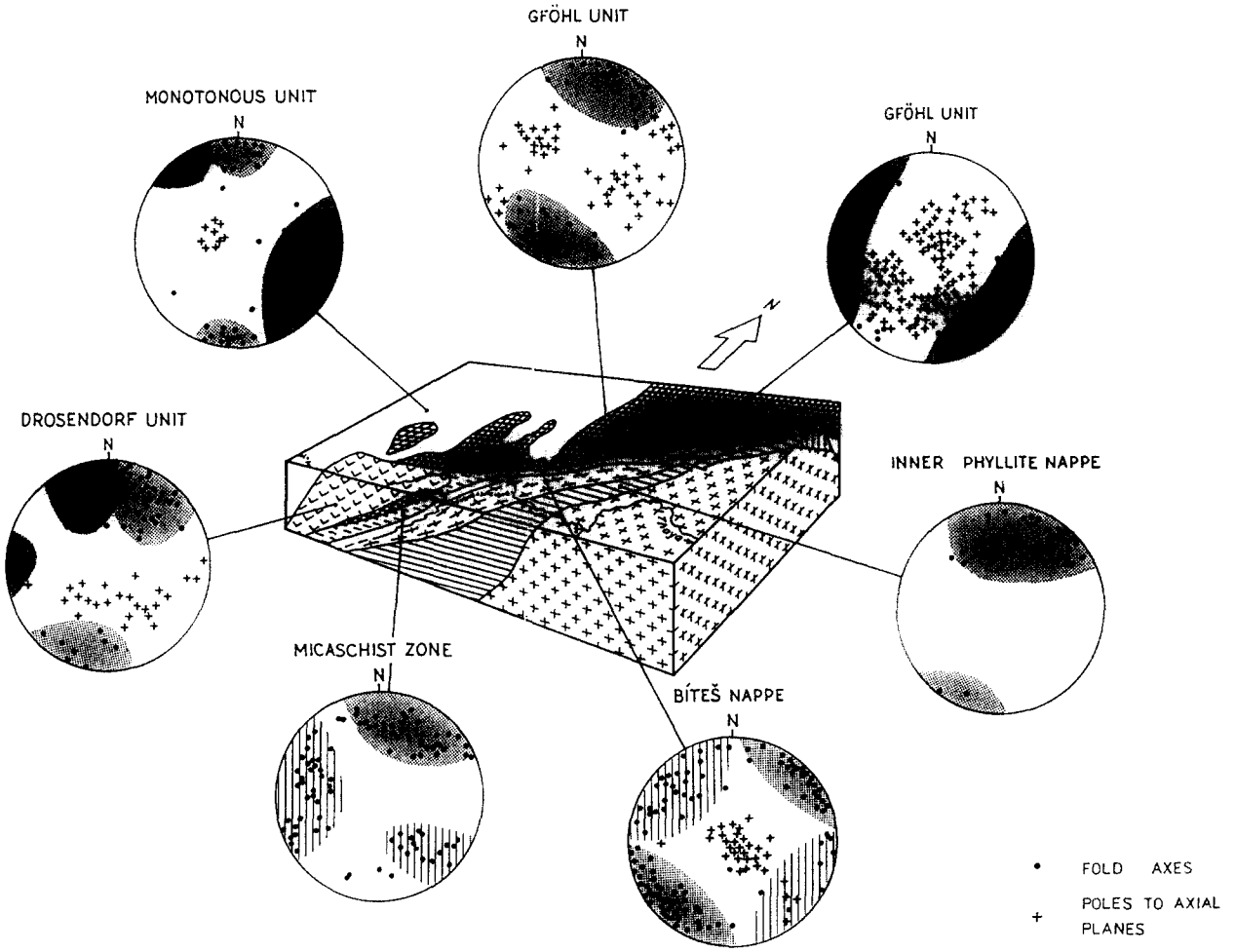

Fig. 5. Orientation diagrams of fold axes (dots) and of poles to axial planes (crosses). Trends of F_1 fold axes (dark-shaded areas in the stereograms) and of F_2 fold axes (light-shaded areas) are indicated. NW-trending F_{2A} fold axes in the micaschist zone and the Bíteš nappe (striped areas) represent slightly non-cylindrical folds with axes perpendicular to the major L_2 stretching lineation that evolve into NE-striking F_{2B} sheath folds. See text for discussion.

mation in the Moldanubicum. Older structures, which would correspond to early NW–SE-trending L_1 in the Moldanubicum, were not observed.

Classical inverted metamorphism is developed in the Moravian zone. In the upper Moravian Bíteš nappe, the S_2 foliation is marked by syn-kinematic garnet, biotite, staurolite and kyanite in metapelites; later, sillimanite grew at the expense of biotite and kyanite. In the lower Moravian Pleissing nappe, S_2 contains syn-kinematic garnet-1 and staurolite-1 (Höck 1975, Höck *et al.* 1990). New inclusion-free garnet-2 (either idiomorphic or forming rims around garnet-1) and staurolite-2 statically overgrew the foliation (Frasl 1983).

In the Bíteš and Weitersfeld orthegneisses, S_2 is marked by strongly recrystallized quartz ribbons, recrystallized feldspar aggregates and flattened biotite flakes. S_2 is concordant with boundaries of individual units (Fig. 3).

An L_2 stretching lineation is marked by pressure shadows around garnet and staurolite in micaschists, and by rodding of quartz–feldspar and biotite aggregates in orthogneisses. It is generally subhorizontal and trends NE–SW, subparallel to the western margin of the Thaya Dome, but oblique to the ENE-trending lithological boundaries at the northern termination of the dome (Fig. 3).

Strain analysis (Fig. 9b) of feldspar aggregates of Bíteš orthogneiss in the Thaya window (Schulmann 1990) show oblate fabrics in the core of the orthogneiss and in the northernmost part of the Thaya dome, associated with well-annealed high-temperature granoblastic microstructures. Plane-strain to constrictional fabrics are typical for the NW-dipping strike-slip domain; textures associated with plane-strain fabrics show later reworking (Schulmann 1990). The intensity of deformation increases in conjunction with the degree of prolateness of strain from the core of the orthogneiss body towards its boundaries; the eastern boundary shows lower strain intensity (Preclik 1926). Deformation of the Weitersfeld orthogneiss at the base of the Pleissing nappe is very homogeneous and is associated with an intense constrictional flow.

Asymmetrical sigmoidal K-feldspar porphyroclasts (Passchier & Simpson 1986) in orthogneisses (Fig. 7c) together with spiral inclusions (Schoneveld 1977) observed in XZ sections of rotated garnets in metapelites (Fig. 8d) indicate a non-coaxial deformation strain history during the Barrovian metamorphic stage. All these

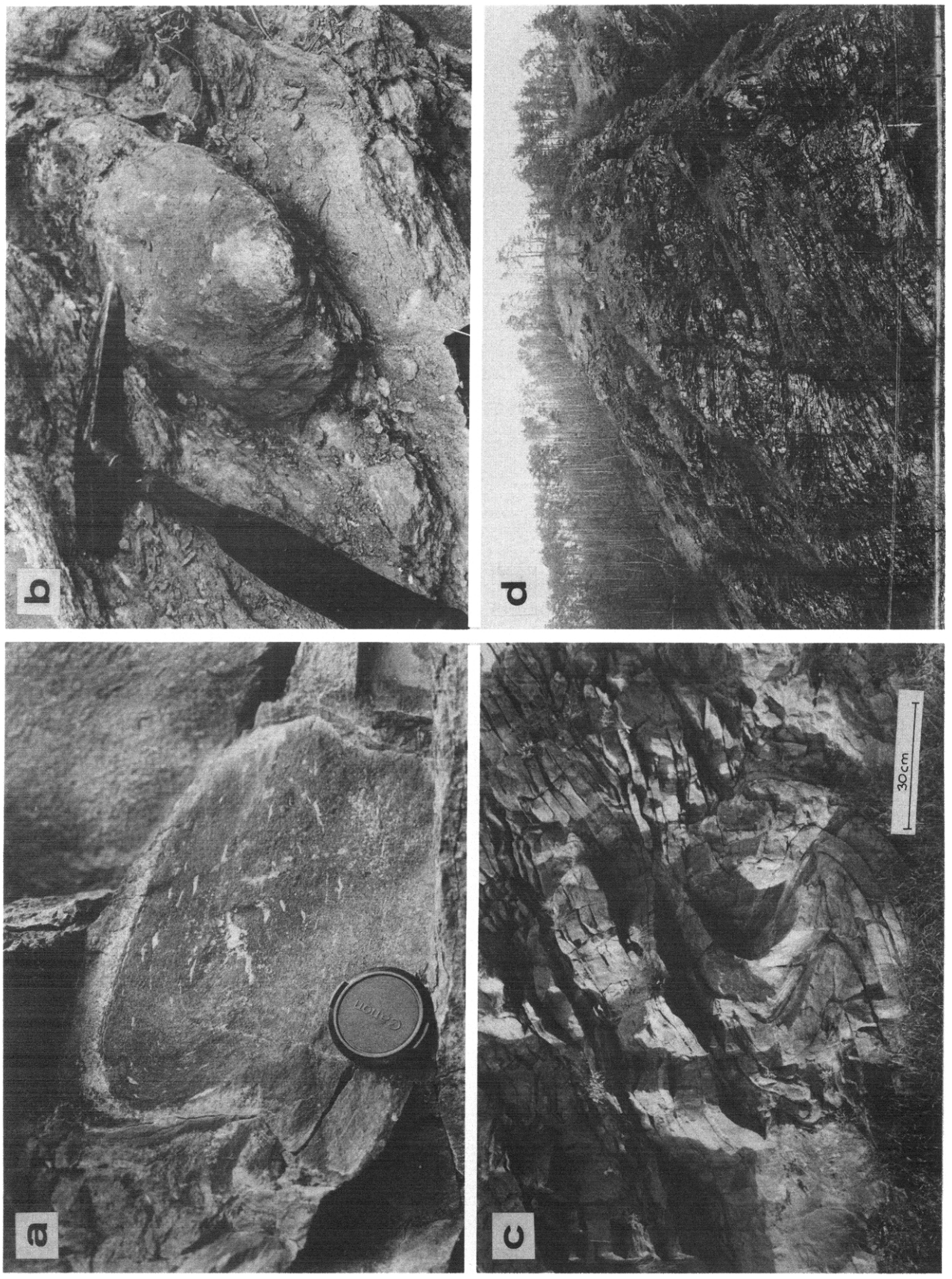

Fig. 6. Types of folds in the studied area. (a) Section through an F_2 sheath fold from the Moldanubicum (Drosendorf nappe). (b) F_2 sheath fold from the Moravicum (Bíteš orthogneiss). (c) W-vergent F_3 folds in Bíteš orthogneiss. (d) Intense F_3 folding in the upper part of the Bíteš orthogneiss.

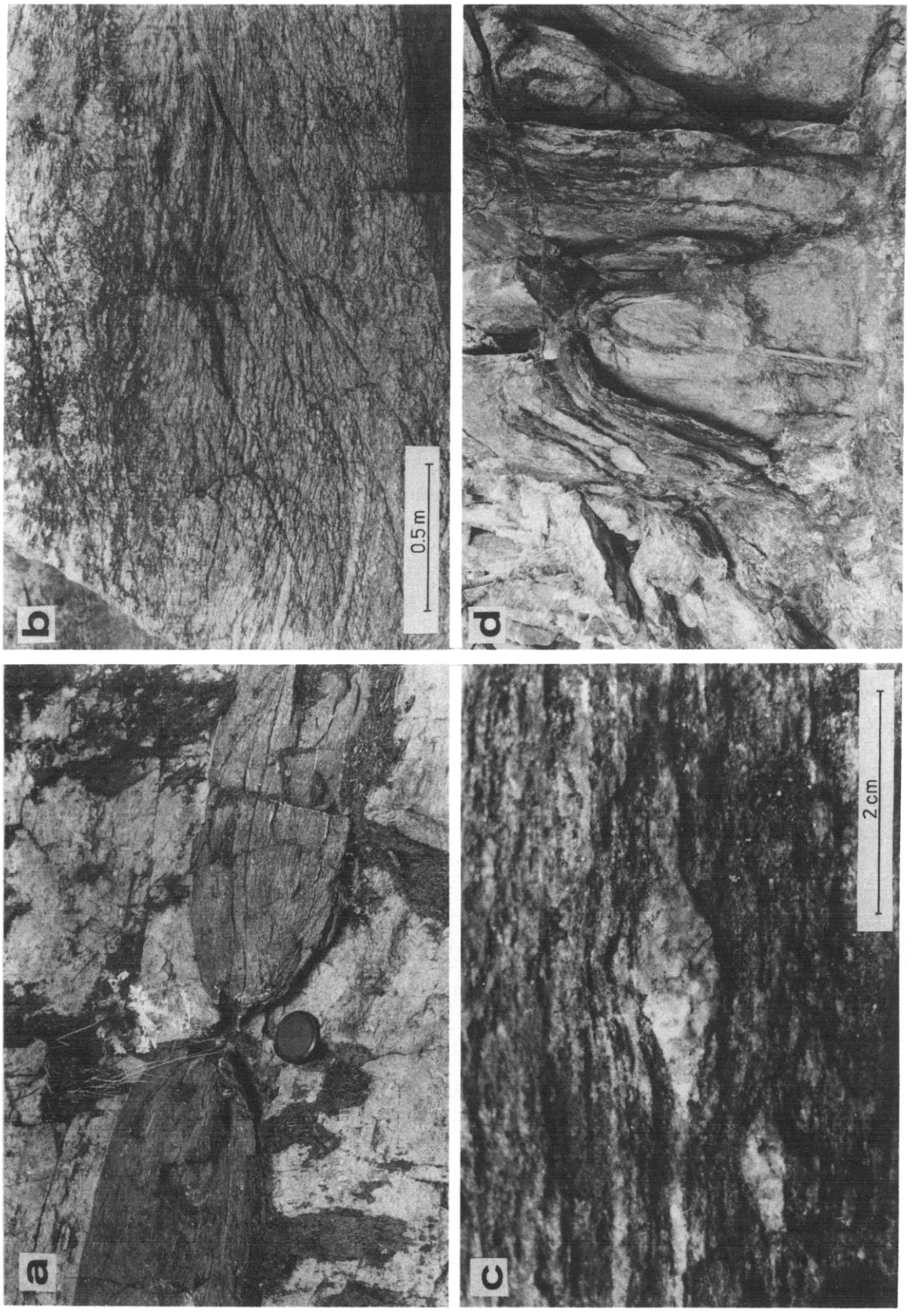

Fig. 7. Examples of mesoscopic structures and sense-of-shear criteria. (a) D_2 boudinage of amphibolite layer in the Moldanubicum (Drosendorf nappe). (b) D_3 normal shear zones in the Moldanubian migmatites. (c) Asymmetric feldspar porphyroclasts in the Bíteš orthogneiss indicating top-to-the-northeast movements. (d) Character of D_2 mylonitization of the marginal part of the Thaya granite; note the shear zone anostomosing around an undeformed granitic pod.

sense-of-shear criteria are consistent with top-to-the-northeast displacement.

Two types of folds have been recognized in the Bíteš and Weitersfeld orthogneisses and their roofs (Kratochvíl & Schulmann 1984, Schulmann 1990): (1) tight to isoclinal recumbent intrafolial F_{2a} folds, with NW–SE-trending axes (Fig. 5) that progressively evolve into (2) medium to strongly non-cylindrical F_{2B} sheath folds with noses oriented parallel to the regional NE–SW-stretching lineation (Figs. 5 and 6b). Both types of folds are close to isoclinal and the fold profile is similar (Ramsay 1967).

D_2 *in the Bruno-Vistulian basement*

The Cadomian basement, including the Thaya granitic complex and its country rock, was heterogeneously reworked during Variscan nappe tectonics. A highly foliated mylonitic belt, some 2–3 km thick, is found at the western edge of the Thaya Massif. Garnet–biotite mineral assemblage grew during D_2 deformation in metapelites of the Thaya granite roof, indicating upper greenschist facies conditions of metamorphism.

A NNE-trending mylonitic S_2 foliation dips steeply (50–70°W) along the western part of the Thaya Dome,

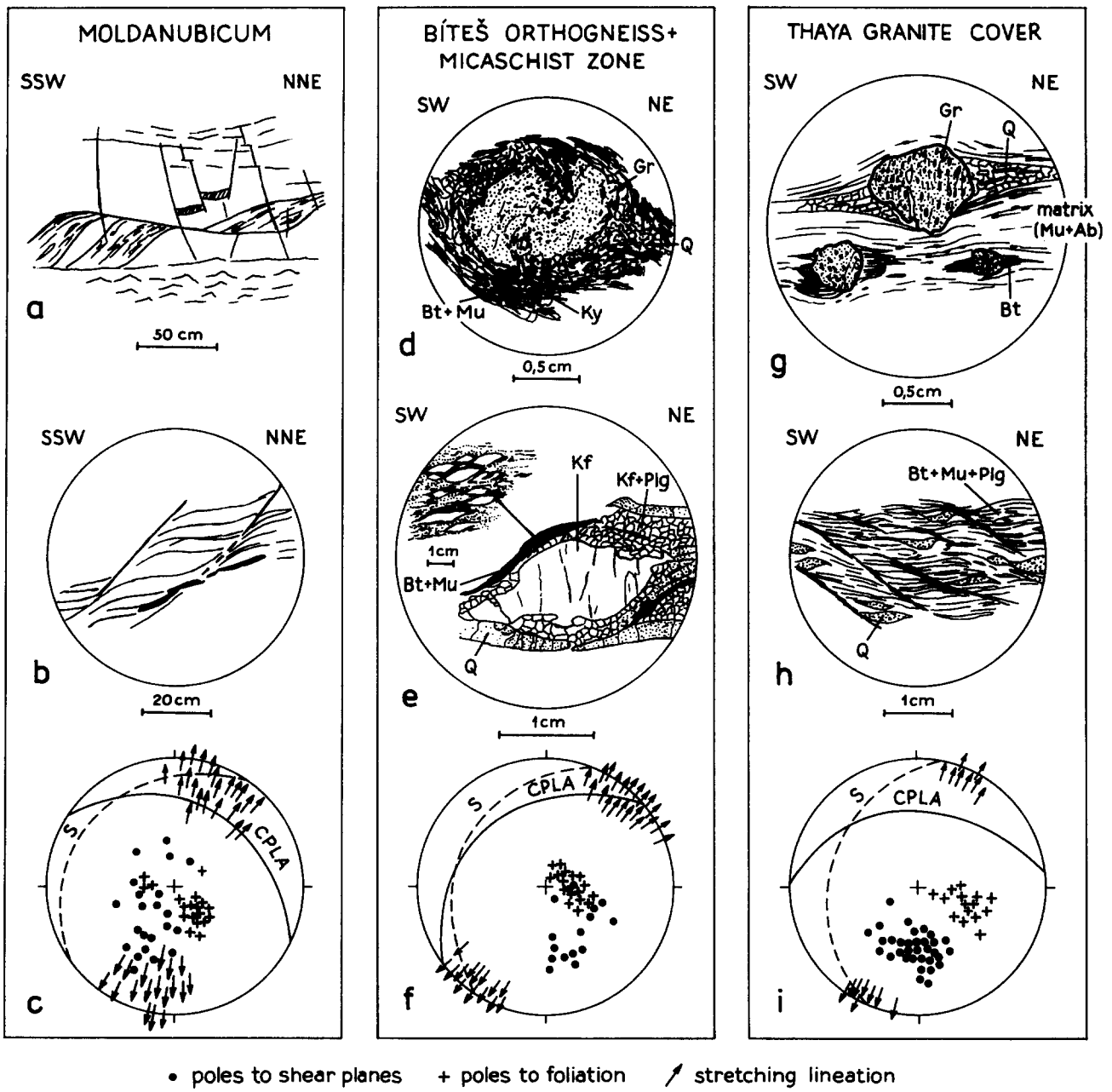

Fig. 8. Kinematic data from Moldanubicum (a, b & c), Moravicum (d, e & f) and the roof of Thaya granite (g, h & i). (a) & (b) show D_3 flat-lying normal shear zones in Moldanubian migmatites. Their orientation is plotted in lower-hemisphere projection (c); (d) & (e) syn-metamorphic D_2 sense-of-shear criteria in the Bíteš nappe indicating top-to-the-northeast shearing. Orientation of shear bands is shown in stereoplot (f); (g) & (h) asymmetric pressure shadows around garnets and D_3 shear bands in the Pleissing nappe with D_3 shear band and lineation orientations shown in stereoplot (i). CPLA, great circle representing best-fit orientation of shear bands; S, great circle representing best-fit foliation plane.

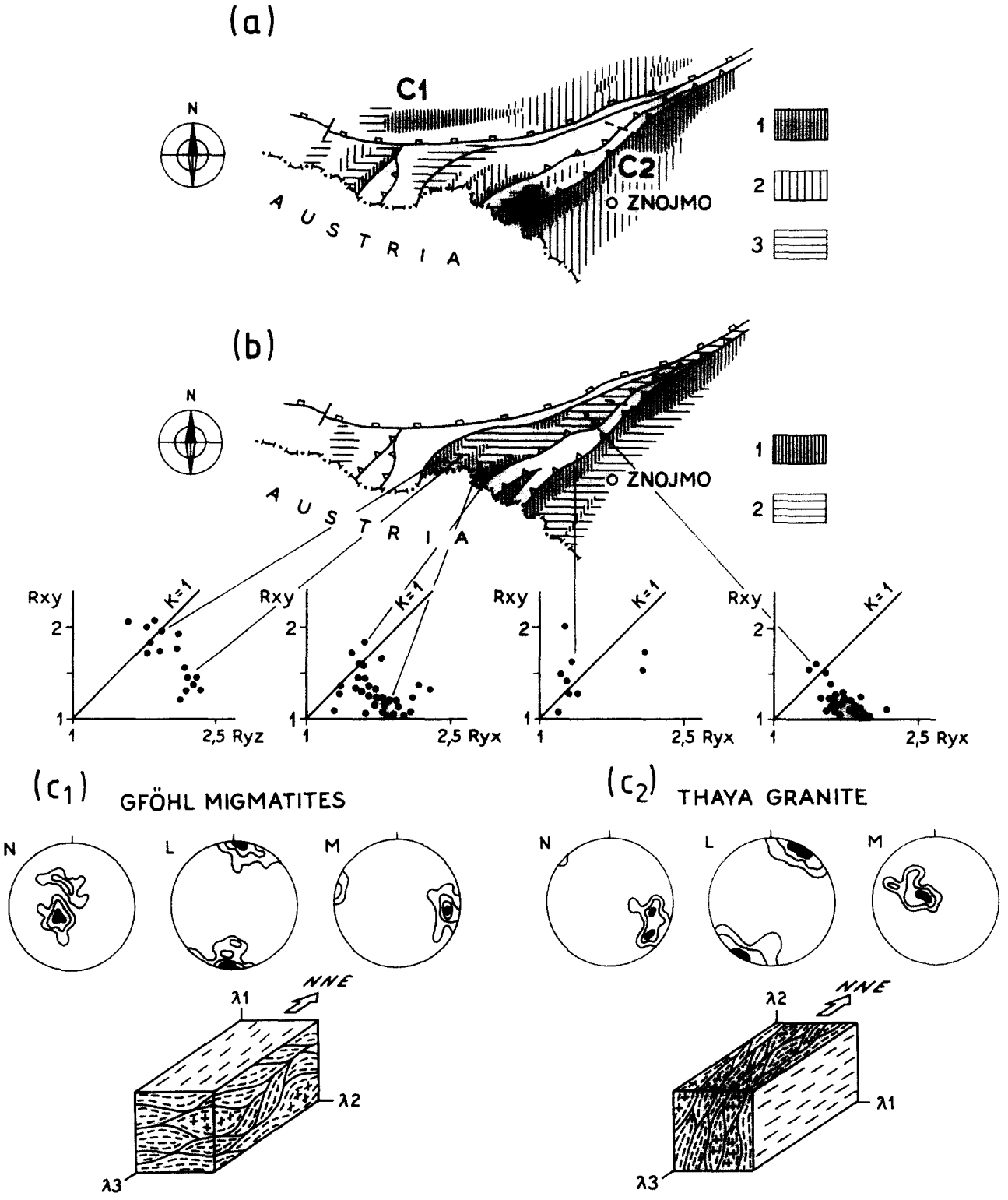

Fig. 9. (a) Map of type and intensity of D_3 reactivation. (a1) Areas of penetrative LT nylonitization (phyllonite and greenschist mylonite); (a2) areas of heterogeneous D_3 deformation—local shear-zone development; (a3) zones of intense F_3 W-vergent folding. (b) Map of regional strain symmetry patterns. (b1) Plane strain to constrictional fabrics; (b2) oblate low-intensity fabrics. Strain data of Schulmann (1990) are displayed on Flinn plots (Flinn 1962). (c) Equal-area projections of N, L and M directions after Gapais *et al.* (1987), together with schematic block diagrams of D_3 shear-zone patterns in Gföhl migmatite (C1) and in Thaya granite (C2). About 50 measurements per diagram, contour intervals 6, 4 and 2% per 1% area.

while at the northern termination the dip decreases to 20–30° (Fig. 3). The foliation is marked by flattened fractured K-feldspar clasts, aggregates formed by destabilization products of plagioclase, quartz ribbons and stable biotite clusters. This microstructure is typical for the brittle–ductile transition during granite mylonitization (Simpson 1985).

A strong NNE-striking stretching lineation L_2 (Fig. 3)

is marked by elongated biotite clusters and dioritic inclusions, and by recrystallized tails around larger feldspar porphyroclasts. Kinematic indicators, such as asymmetrical pressure shadows around feldspar clasts (Passchier & Simpson 1986), mica fish (Lister & Snoke 1984) and asymmetrical pull-apart boudinage of plagioclase and K-feldspar (Hanmer 1986) indicate top-to-the-north-northeast movement.

Prolate fabrics dominate at the contact with the overlying Pleissing nappe (Fig. 9b). Further east the deformation becomes inhomogeneous and large volumes of isotropic granite are preserved within sheared rock (Fig. 7d). Zones of homogeneously foliated orthogneiss anastomose around lense-shaped pods of undeformed granite elongated in NE–SW direction. Foliation perturbations around low-strain domains are generally minor and dip steeply to the northwest (Fig. 9c2). According to Choukroune & Gapais (1983), a low angle between shear zones is in agreement with relatively high-temperature deformation.

D_3 AND REACTIVATION OF THE NAPPE PILE

Low-grade reactivation of the Moldanubian–Moravian nappe pile is ascribed to a D_3 event. It is related to a strong non-coaxial northeast extension, marked by deformation of brittle–ductile and brittle shear zones and of asymmetrical 'A-folds' (Malavieille 1987). Major shearing is concentrated in a zone of lithological weakness within the paragneiss which surrounded the Thaya granite and corresponds to the reactivation of D_2 mylonitic fabrics. The attribution of structures in different units to one D_3 tectonic event is justified by: (1) the retrogressive character of structures; (2) the extensional character of the deformation with; (3) a common orientation of the principal extension direction.

D_3 *in Moldanubian nappes*

The intensity of D_3 deformation is very heterogeneous. In isotropic diatexites local retrograde shear zones grade into completely gneissified *S–C* mylonites (Fig. 7b), while in non-migmatized well-foliated schists D_3 folding prevails (Schulmann *et al.* 1992).

In isotropic migmatite, brittle–ductile conjugate NE- or SW-dipping normal shear zones with opposite shear sense are characteristic (Figs. 8 and 9c1). Intense mylonitic S_3, synchronous with greenschist-facies metamorphism (chlorite–muscovite), is marked by a preferred orientation of grains and anastomoses around low-strain lenses (Ramsay & Allison 1979, Choukroune & Gapais 1983, Simpson 1983, Gapais *et al.* 1987). S_3 dips gently (30°) to the northeast. The L_3 stretching lineation is very intense and plunges 10–25°NNE (Figs. 3 and 9c). Several shear-sense criteria, e.g. *S–C* fabrics (Berthé *et al.* 1979), shear bands (Platt & Vissers 1980) and asymmetric pull-apart boudinage (Hanmer 1986) demonstrate top-to-the-northeast sense of displacement.

The overall geometric pattern of the shear zones is shown in L, M and N diagrams of Gapais *et al.* (1987) in Fig. 9(c1). Poles to N planes tend to concentrate in two unequally populated maxima in the $(\lambda_1 - \lambda_3)$ plane at a low angle to λ_3. Shear directions L tend to cluster around the λ_1 direction and poles to M planes (Arthaud 1969) are concentrated around λ_2. Such asymmetric patterns indicate a non-coaxial deformation history, marked by a predominantly top-to-the-northeast shear sense during an extensional shear regime (Gapais *et al.* 1987).

In anisotropic non-migmatized schists reactivation is marked by intense F_3 folding, forming a set of small- to medium-scale folds which deform the S_1 metamorphic foliation, L_1 and F_1 folds. Axes of F_3 folds trend NNE–SSW parallel to L_3 and axial surfaces of F_3 folds are roughly parallel to shear planes of D_3 shear zones in migmatite. The folds are flexural, gentle to open with rounded shapes.

F_3 folding has a different character in the Drosendorf nappe. The axes of F_3 folds plunge to the northeast at shallow to steep angles (10–60°) and the corresponding axial planes dip to the northwest at intermediate to steep angles (30–60°) (Fig. 5). Kratochvíl & Schulmann (1984) have shown that axes of close flattened folds tend to be subhorizontal while axes of open flexural folds tend to be subvertical, axial planes in both cases being the same. This steepening of fold axes in the Drosendorf nappe may be explained using the model of fold development in a wrench zone by Odonne & Vialon (1983). According to this model the intensity of folding decreases, accompanied by steepening of fold axis plunge, with increasing distance from the central part of the wrench zone.

In order to compare the deformation pattern of D_3 brittle–ductile normal shear zones with that of sets of microfaults concentrated within lenses of undeformed migmatite, an attempt was made to determine the principal-stress-direction axes from the microfaults. The geometry of microfaults is generally consistent with that of shear zones and indicates an extensional regime. Analysis of slickenside surfaces was carried out by computer procedure (modification of the method of Carey & Brunier, 1974) in about 20 sites (Fig. 10). In the first stage of computer processing an average stress tensor was calculated from the entire measured set of microfaults and striations. This average stress tensor was then applied on the measured set of microfaults and orientations of corresponding theoretical striations on individual faults were determined. The numerical procedure compares the orientations of both theoretical and measured striations and selects a best-fitting set of measured microfaults, which correspond well to the average tensor (Angelier 1989). Figure 10 shows that the directions of σ_3 axes are concentrated along the $\lambda_1 - \lambda_3$ plane with maximum at about 20° from the λ_1 direction. Corresponding σ_1 and σ_2 axes tend to define a small circle centered about the mean σ_3 axis.

Results of microfault analysis reveal similar orientation of principal stress axes σ_1, σ_2 and σ_3, with corresponding λ_1, λ_2 and λ_3 axes inferred from brittle–ductile

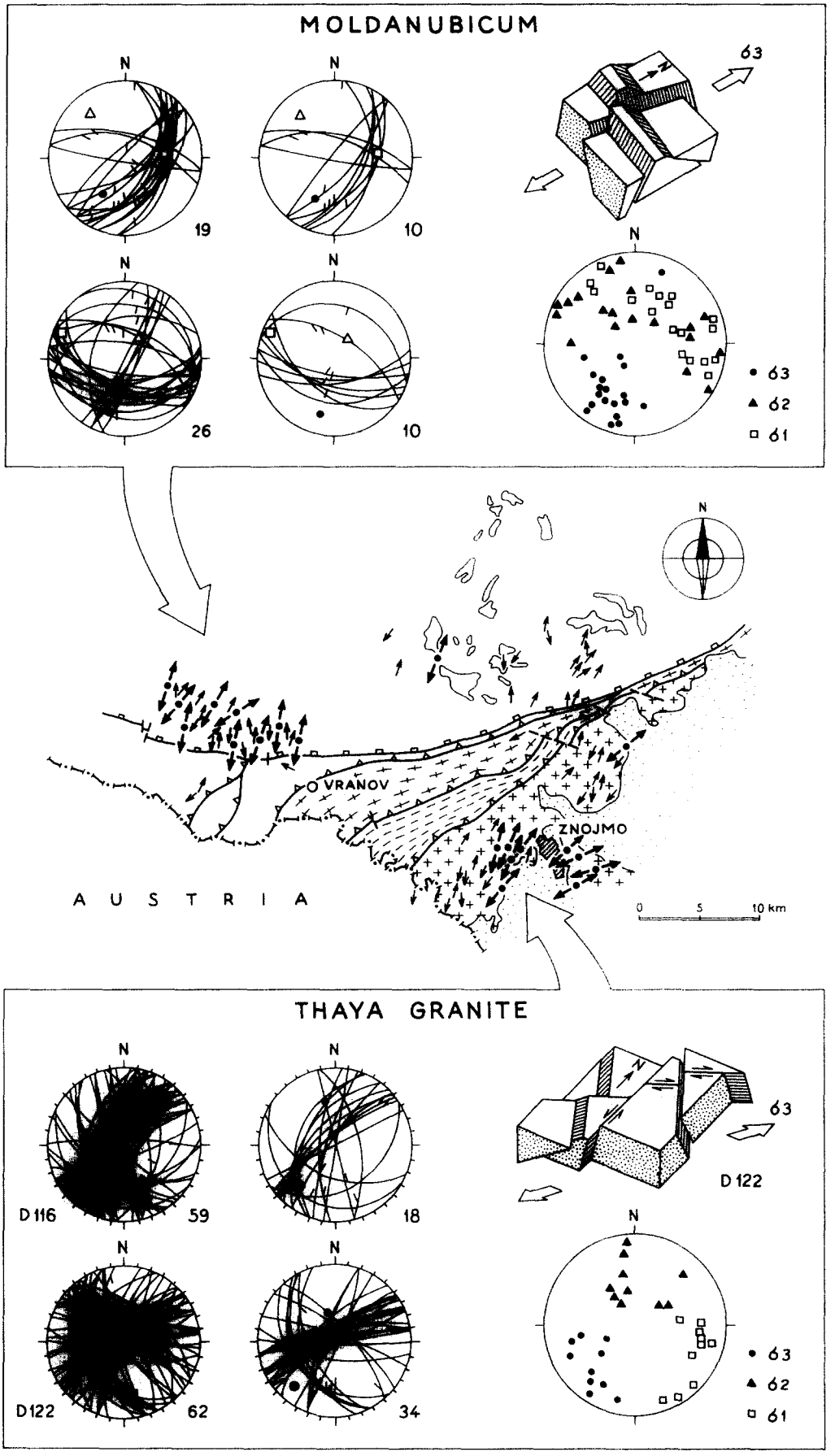

Fig. 10. Structural sketch map showing L_3 lineations (thin arrows) in the Moldanubian zone and Thaya granite, and trends of extensional directions calculated from microfault arrays (solid arrows). Insets show stereographic projections of two typical examples of striated faults from the Moldanubicum rocks and the Thaya granite: measured set on the left and selected set calculated using numerical procedure in the center of the insets. See text for explanation. Synoptic plots (lower right in insets) show calculated principal axes of stress ellipsoids from 19 stations in Moldanubicum and 10 sites in Thaya granite. Schematic block diagrams show activity of principal fault systems. See text for discussion.

shear zone patterns. This may indicate continuous kinematic evolution passing from brittle–ductile to brittle conditions.

D_3 *in the Moravian nappe pile*

In Moravian nappes, D_3 deformation is characterized by formation of retrograde mylonitic shear zones, either along earlier lithotectonic boundaries (e.g. the base of Bíteš and Pleissing nappes), or affecting inner parts of individual lithological units, and by intense folding of primary intrusive sills at the roof of the Bíteš and Weitersfeld orthogneisses.

The D_3 mylonitic shear zones are recognized by reactivation of the early medium-temperature foliation and by destabilization of earlier mineral assemblages. The marble and calc-silicate rock in the upper part of Pleissing nappe were imbricated together with the base of the Bíteš orthogneiss body during the D_3 phase.

The characteristic mineral assemblage of D_3 deformation is the growth of new muscovite and chlorite, and the breakdown of biotite and oligoclase (Bernroider 1986). Large amounts of sericite grow on S_3 foliation planes. An L_3 is marked by the corrugation of S_{2-3} planes, by flattened chloritized biotite and the linear arrangement of sericite. Distinct NNE-dipping shear bands suggest a general NNE sense of shearing.

The roofs of the Bíteš and Weitersfeld orthogneiss bodies, rich in orthogneiss sheets cutting overlying metasedimentary formations, represent mechanically strongly anisotropic regions that were intensely folded during D_3 (Fig. 6d). Northeast-trending recumbent W-vergent F_3 folds on a metre scale with subhorizontal axial planes (Fig. 6c) were formed. These open to closed folds have variable shape and mostly rounded hinges.

D_3 *deformation in the Bruno-Vistulian basement*

Metasedimentary country rock of the Thaya massif shows strong D_3 mylonitization along the phyllonitic zone associated with décollement of most of the mantle rocks from the Thaya granite. Such homogeneously retrogressed and phyllonitized mica-schist can locally be as much as 1 km wide.

Phyllonitization is characterized by an occurrence of fine-grained chlorite–sericite–albite phyllite with a large number of quartz lenses that are mostly found in the neck zones of foliation boudinage. The alternation of chlorite–sericite phyllite with biotite schist has been interpreted as a result of the imbrication of the Thaya granite country rock below the Pleissing nappe (Preclik 1926).

Ubiquitous NNE-dipping C' surfaces are consistent with a NNE-directed sense of shearing parallel to L_3 (Figs. 8h & i). Helicitic inclusions in rotated garnets are commonly disrupted by late shear surfaces at the boundaries with the fine-grained matrix, and asymmetric pressure shadows around garnets are filled by chlorite and quartz. All these criteria indicate that the garnets are pre-tectonic with respect to D_3.

D_3 deformation in the autochtonous granite is manifested by subvertical NNE–SSW-trending brittle–ductile S_3 shear zones, producing fine-grained ultramylonites and phyllonites (Fig. 9c2). These zones either cut the S_2 mylonitic foliation of previously deformed granite in the marginal mylonitic zone of the batholith or heterogeneously affect isotropic granite in the core. Poles to shear planes (N) (Gapais *et al.* 1987) form an elongated maximum in the $(\lambda_3 - \lambda_1)$ plane. Shear directions (L) cluster in the λ_1 direction and poles to M planes form an elongated maximum in the $(\lambda_2 - \lambda_3)$ plane perpendicular to the mean shear direction. There is only one dominant set of shear zones associated with NE-directed displacement. According to Gapais *et al.* (1987) this shear zone pattern may be interpreted as a result of non-coaxial deformation during dextral wrenching.

Sets of striated microfaults associated with D_3 shear zones have been used for palaeostress determinations at 10 stations (Fig. 10). Calculated σ_3 axes of the stress ellipsoid trend SW–NE and σ_1 axes of maximum compression are subparallel to λ_3. These data are fully compatible with the orientation of extension and compression directions linked to brittle–ductile subvertical deformation zones (Fig. 9c2). The brittle deformation and brittle–ductile shear zones are thus connected to the same dextral wrenching regime that prevailed during D_3 deformation of the Thaya granite.

DISCUSSION AND CONCLUSIONS

Nappe stacking in the studied area was a polyphase process, which implies progressive modification of the strain regime through time and progressive downward migration of thrust planes (Fig. 11).

The early stacking D_1 (i.e. creation of the Moldanubian nappe pile) is characterized by a dominantly high-temperature deformation history and by uplift of deep crustal and mantle rocks. The resulting flat-lying foliation bears a NW–SE-stretching lineation that provides evidence for the direction of movement. Rootless F_1 folds have widely dispersed fold-axis orientations. The thrusting probably took place during Late Devonian to Early Carboniferous times (Van Breemen *et al.* 1982, Matte *et al.* 1990).

After D_1 the Moldanubian nappe pile was probably obliquely stacked over the Moravian foreland. This stage corresponds to the D_2 deformation phase. The development of Barrovian metamorphism in the Moravian and lower Moldanubian (Drosendorf) nappes is associated with a change in finite-strain-axes orientation and with northeasterly directed thrusting and wrenching (transpressional tectonics). The subsequent stacking of Moravian nappes led to medium-temperature mylonitization of the western margin of the autochthonous Thaya granite.

The Moravian nappes have been translated along and partially thrust over the lateral ramp of the Cadomian basement during D_2. Oblate fabrics occur in overthrust parts of the Moravian nappes that lie flat over the

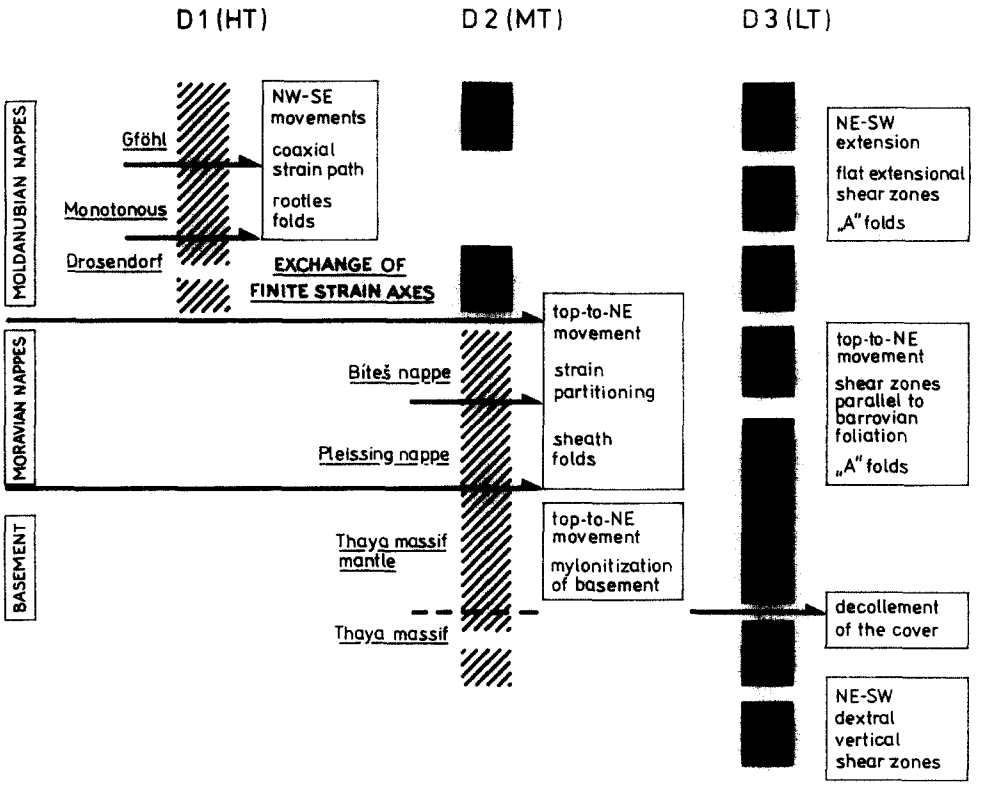

Fig. 11. Scheme of progressive stacking along the southeastern margin of the Bohemian Massif showing main features of individual deformational phases. Note the migration of deformation in time and space. Striped columns indicate prograde syn-metamorphic shear deformation. Black columns show domains affected by structural reactivation. Thrust–wrench boundaries are indicated by arrows.

basement. In contrast, large-scale strain partitioning took place in those parts of the Moravian nappes that moved laterally along the ramp. Non-coaxial plane strain to constrictional fabrics are located at the boundaries of individual units, whereas oblate fabrics are preserved in their cores. An interesting feature that is difficult to explain is the systematically constrictional character of fabrics in the whole upper mylonitized part of the Thaya Massif. Such a variation in strain symmetry and intensity is most probably related to the curved shape of the Thaya basement, with its westerly strike-slip domain and easterly flat–thrust domain.

F_2 sheath folds (Figs. 6a & b) and isoclinal syn-schistose folds developed in areas with strong lithological anisotropy, e.g. in the upper intrusive contacts of the Bíteš and the Weitersfeld orthogneisses, and in layered amphibolites at the base of the Drosendorf nappe. The finite-strain symmetry in these areas is of the plane-strain to constrictional type and the axes of the F_2 folds are parallel to L_2 stretching. We suggest that these folds originated as a result of intense non-coaxial shearing in anisotropic rocks during ductile northeastward D_2 movement. According to recent geochronological investigations, the D_2 phase occurred between 350 and 340 Ma (Dallmeyer *et al.* 1990).

The oblique collision of the stacked Moldanubian–Moravian nappe pile continued with a lateral ramp effect along the Bruno-Vistulian Cadomian block and its sedimentary cover. This led to the décollement and strong phyllonitization of the metasedimentary envelope of the Thaya Massif. The autochtonous block was reworked along steeply-inclined dextral brittle–ductile shear zones under greenschist facies metamorphism, while the whole nappe pile was overthrust towards the north-northeast. The Moravian nappes are sheared by low-temperature mylonite zones that are parallel to the early metamorphic foliation. In contrast, at the top of the nappe pile the uppermost part of the Gföhl nappe was reactivated in flat, extensional normal brittle–ductile shear zones. D_3 deformation was in all cases non-coaxial and of plane strain symmetry.

F_3 W-vergent folds are post-metamorphic and occur throughout the whole nappe pile, including the Gföhl nappe. The F_3 folds may have resulted from foliation-parallel extensional northeastward shearing of layered sequences that initially dipped to the northwest (Schulmann 1990, Schulmann *et al.* 1991). This geometry might produce the observed northwestward overturning of the folds (Figs. 6c & d). We interpret F_3 folds as typical 'A-folds' in the sense of Malavieille (1987). Such an interpretation may solve the problem of the northwest vergency of F_3 folds, which is in conflict with supposed E-vergent Moldanubian overthrusting (Dudek 1962).

The intensity of F_3 folding progesssively decreases from the lower units towards the upper Moldanubian nappes. At the same time, orientation of the fold axes progressively steepens, with fold axis pitch changing from 0–15° in Moravicum to 60° in the Drosendorf nappe. This agrees with the theoretical model of Odonne & Vialon (1983), describing the decrease in folding intensity accompanied by steepening of fold axes plunge, with increasing distance from the core of large-

scale transcurrent zone. F_3 folds with subhorizontal fold axes and subhorizontal axial planes are related to an extensional shear regime, that predominated in the uppermost Gföhl nappe during D_3.

XY planes of D_3 strain ellipsoids in basement and the uppermost Gföhl nappe are mutually perpendicular, but the X axes and shearing vectors remain constantly NE–SW trending. We suggest that both the Moravian zone and the Drosendorf nappe have been reactivated by large-scale transcurrent movement along the Thaya lateral ramp during the D_3 regime, while in the uppermost Gföhl nappe an extensional regime predominated. According to geochronological data, this event is constrained between 330 and 320 Ma (Maluski personal communication, Dallmeyer *et al.* 1990). Similar combination of transverse and transcurrent extensional tectonics was reported from the Montagne Noire area of the Variscan chain (Echtler & Malavieille 1990). In the Thaya Dome, the location of the transcurrent fault system was mechanically controlled by the basement geometry.

Acknowledgements—We would like to thank the Ministry of Environment of the Czech Republic for research support (grant No. HS 140). Bureau de Recherches Géologiques et Minières and Professor P. Magne (French Embassy in ČSFR) helped to facilitate the financial support. Constructive suggestions by C. Passchier, P. Heitzmann and an anonymous reviewer improved the text significantly. Š. Novák drew all the figures.

REFERENCES

Angelier, J. 1989. From orientation to magnitudes in paleostress determinations using fault slip data. *J. Struct. Geol.* **11**, 37–50.

Arthaud, F. 1969. Méthode de détermination graphique des directions de raccourcissement, d'allongement et intermédiaire d'une population de failles. *Bull. Soc. géol. Fr.* **11**, 729–737.

Bernroider, M. 1986. Zur Geologie und Petrographie Moravischer Gesteine im Gebiet NW Weitersfeld, Niederosterreich. Unpublished dissertation, University of Salzburg.

Berthé, D., Choukroune, P. & Jegouzo, P. 1979. Orthogneiss, mylonite and non-coaxial deformation of granites: the example of the South Armorican Shear zone. *J. Struct. Geol.* **1**, 31–42.

Carey, E. & Brunier, B. 1974. Analyse théorique et numérique d'un modèle mécanique élémentaire appliqué à l'étude d'une population de failles. *C. r. Acad. Sci. Paris* **279**, 891–894.

Choukroune, P. & Gapais, D. 1983. Strain pattern in the Aar granite (Central Alps): orthogneiss developed by bulk inhomogeneous flattening. *J. Struct. Geol.* **5**, 411–418.

Cobbold, P. R. & Quinquis, H. 1980. Development of sheath folds in shear regimes. *J. Struct. Geol.* **2**, 119–126.

Dallmeyer, D., Neubauer, F. & Höck, F. 1990. $^{40}Ar/^{39}Ar$ mineral age controls on the chronology of late-Paleozoic tectonothermal activity in the southeastern Bohemian massif, Austria (Moldanubian and Moravosilesian zone). In: *Fieldguide to IGCP 233 Conference on Paleozoic Orogens in Central Europe—Geology and Geophysics*. IGCP, Göttingen.

Dudek, A. 1960. Kristallinische Schiefer und Devon östlich von Znojmo (Znaim). *Sbor. ÚÚG* **26**, 101–141.

Dudek, A. 1962. Zum Problem der moldanubischen Überschiebung im Nordteil der Thayakuppel. *Geologie* **11**, 757–792.

Dudek, A. 1980. The crystalline basement block of the Outer Carpathians in Moravia—Brunovistulicum. *Rozpr. Čs. Akad. věd. ř. mat. přír.* **90**, 8.

Echtler, H. & Malavieille, J. 1990. Extensional tectonics, basement uplift and Stephano-Permian collapse basin in a late Hercynian Metamorphic core complex from the French Massif Central (Montagne Noire). *Tectonophysics* **177**, 125–138.

Flinn, D. 1962. On folding during three dimensional progressive deformation. *Q. J. geol. Soc. Lond.* **118**, 358–428.

Frasl, G. 1983. Zur Geologie des Kristallins und Tertiärs der weiteren Umgebung von Eggenburg. Excursion Guide, Österreichische Geol. B.-A. 1983.

Frasl, G., Fuchs, G., Matura, A. & Thiele, O. 1977. Einführung in die Geologie des Waldviertel Grundgebirges. In: *Arbeitstagung der Geologischen Bundesanstalt* (edited by Geol. Bundesanstalt). Spec. Publ. *Austr. Geol. Surv. Wien.*

Frasl, G., Höck, V. & Finger, F. 1990. The Moravian zone in Austria. In: *Fieldguide—Bohemian Massif, International Conference on Paleozoic Orogens in Central Europe*. Project 233, IGCP, Göttingen.

Gapais, D. 1989. Les orthogneiss; structures, mecanismes de déformation et analyse cinématique. *Mém. docum. CAESS*, **28**.

Gapais, D., Bale, P., Choukroune, P., Cobbold, P. -R., Mahjoub, Y. & Marquer, D. 1987. Bulk kinematics from shear zone patterns: some field examples. *J. Struct. Geol.* **9**, 419–427.

Hájek, T. 1990. The mantle rocks of the Dyje massif and their relation to the Moravicum and Brunovistulicum. *Čas. Min. Geol.* **35**, 251–259.

Hanmer, S. 1986. Asymmetrical pull-aparts and foliation fish as kinematic indicators. *J. Struct. Geol.* **8**, 111–122.

Höck, V. 1975. Mineralzonen in Metapeliten und Metapsammiten der Moravischen Zone in Niederösterreich. *Mitt. Geol. Gesell.* **66–67**, 49–60.

Höck, V., Marschallinger, R. & Topa, D. 1990. P-T Evolution in metapelites of the Moravian zone of Austria. In: *Conference Abstracts. International Conference on Paleozoic Orogens in Central Europe*. Project 233, IGCP, Göttingen.

Jenček, V. & Dudek, A. 1971. Beziehungen zwischen dem Moravikum und Moldanubikum am Westrand der Thaya-Kuppe, *Věst. ÚÚG* **46**, 331–338.

Johan, V., Autran, A., Ledru, P., Lardeaux, J.-M. & Melka, R. 1990. Discovery of relics of high pressure metamorphism at the base of the Moldanubian nappe complex. In: *Conference Abstracts. International Conference on Paleozoic Orogens in Central Europe*. Project 233, IGCP, Göttingen.

Kratochvíl, M. & Schulmann, K. 1984. Correlation of the Moravicum and Moldanubicum in the Dyje valley on the basis of structures of polyphase deformation. *Čas. Min. Geol.* **29**, 337–352.

Lardeaux, J.-M., Johan, V., Autran, A. & Ledru, P. 1991. Talc–phengite–kyanite bearing metapelites: high-pressure metamorphism in the Moravian zone and its tectonic significance. In: *Conference Abstracts. Geological Workshop Moravian Windows, Moravský Krumlov*.

Lister, G. S. & Snoke, A. W. 1984. S–C mylonites. *J. Struct. Geol.* **6**, 617–638.

Malavieille, J. 1987. Extensional shearing deformation and kilometer-scale "a" type folds in a cordilleran metamorphic core complex (Raft River Mountains, NW Utah). *Tectonics* **6**, 423–448.

Matějovská, O. 1975. The Moldanubian gneiss series of south-western Moravia and its relation to granulites. *Věst. ÚÚG* **50**, 345–351.

Matte, Ph., Maluski, H., Rajlich, P. & Franke, W. 1990. Terrane boundaries in the Bohemian massif: result of large scale Variscan shearing. *Tectonophysics* **177**, 151–170.

Medaris, L. G. Jr., Wang, H. F., Mísař, Z. & Jelínek, E. 1990. Thermobarometery, diffusion modelling and cooling rates of crustal garnet peridotites: Two examples from the Moldanubian zone of the Bohemian Massif. *Lithos* **25**, 189–202.

Morauf, W. & Jäger, F. 1982. Rb–Sr whole rock ages for Bíteš Gneiss, Moravicum, Austria. *Terra Cognita* **2**, 60–61.

Odonne, F. & Vialon, P. 1983. Analogue models of folds above a wrench fault. *Tectonophysics* **99**, 31–46.

Passchier, C. W. & Simpson, C. 1986. Porphyroclast systems as kinematic indicators. *J. Struct. Geol.* **8**, 831–843.

Platt, J. P. & Vissers, R. L. M. 1980. Extensional structures in anisotropic rocks. *J. Struct. Geol.* **2**, 397–410.

Preclik, K. 1925. Zur Analyse des Moravischen Faltenwurfes im Thayatale. *Verh. Geol. B.-A.* **1924**, 180–192.

Preclik, K. 1926. Das Nordende der Thayakuppel. *Sbor. SGÚ* **6**, 373–398.

Rajlich, P. 1987. Variszische duktile Tektonik im Böhmischen Massiv. *Geol3 Rdsch.* **76**, 755–786.

Ramsay, J. G. 1967. *Folding and Fracturing of Rocks*. McGraw-Hill, New York.

Ramsay, J. G. & Allison, I. 1979. Structural analysis of shear zones in alpinised Hercynian granite. *Schweiz. miner. petrogr. Mitt.* **59**, 251–279.

Sander, B. 1911. Über Zusammenhänge zwischen Teilbewegung und Gefüge in Gesteinen. *Miner. petrogr. Mitt.* **30**, 281–315.

Sander, B. 1930. *Gefügekunde der Gesteine*. Vienna.

Scharbert, S. 1977. Neue Ergebnisse radiometrischer Altersbestimmungen an Gesteinen des Waldviertels. *Arbeitstag. Geol. B.-A.* 10–13.

Scharbert, S. & Batík, P. 1985. The age of the Thaya (Dyje) pluton. *Verh. Geol. B. -A.* **3**, 325–331.

Schoneveld, Ch. 1977. A study of some typical inclusion patterns in strongly paracrystalline garnets. *Tectonophysics* **39**, 453–471.

Schulmann, K. 1990. Fabric and kinematic study of the Bíteš orthogneiss (southwestern Moravia): Result of large-scale northeastward shearing parallel to the Moldanubian/Moravian boundary. *Tectonophysics* **177**, 229–244.

Schulmann, K., Ledru, P., Autran, A., Melka, R., Lardeaux, J. M., Urban, M. & Lobkowicz, M. 1991. Evolution of nappes in the eastern margin of the Bohemian Massif: a kinematic interpretation. *Geol. Rdsch.* **80**, 73–92.

Schulmann, K., Matějovská, O. & Melka, R. 1992. Kinematics of Variscan shear deformation on Moldanubian polymetamorphic complex. In: *Proceedings of the International Conference on 'Bohemian massif'*. Czech Geological Survey, Prague, 233–246.

Simpson, C. 1983. Strain and shape fabric variations associated with ductile shear zones. *J. Struct. Geol.* **5**, 61–72.

Simpson, C. 1985. Deformation of granite rocks across the brittle–ductile transition. *J. Struct. Geol.* **7**, 503–511.

Suess, F. E. 1912. Die moravischen Fenster und ihre Beziehung zum Grundgebirge des Hohen Gesenkes. *Denkschr. Österr. Akad. Wiss., math.-naturwiss.* **88**, 541–631.

Suess, F. E. 1926. *Intrusionstektonik und Wandertektonik im variszischen Grundgebirge*. Borntrager, Berlin.

Van Breemen, O., Aftalion, M., Bowes, D. R., Dudek, A., Mísař, Z., Povondra, P. & Vrána, S. 1982. Geochronological studies of the Bohemian massif, Czechoslovakia, and their significance in the evolution of Central Europe. *Trans. R. Soc. Edinb. Earth Sci.* **73**, 89–108.

Waldmann, L. 1930. Zum geologischen Bau der Thayakuppel und ihre Metamorphose. *Mitt. geol. Ges. Wien* **21**, 133–152